

Cite this: *Chem. Sci.*, 2021, 12, 12610

All publication charges for this article have been paid for by the Royal Society of Chemistry

Received 20th July 2021  
Accepted 13th August 2021

DOI: 10.1039/d1sc03957a

rsc.li/chemical-science

# Nitride protonation and NH<sub>3</sub> binding *versus* N–H bond cleavage in uranium nitrides†

Megan Keener,<sup>1</sup> Rosario Scopelliti<sup>2</sup> and Marinella Mazzanti<sup>1\*</sup>

The conversion of metal nitrides to NH<sub>3</sub> is an essential step in dinitrogen fixation, but there is limited knowledge of the reactivity of nitrides with protons (H<sup>+</sup>). Herein, we report comparative studies for the reactions of H<sup>+</sup> and NH<sub>3</sub> with uranium nitrides, containing different types of ancillary ligands. We show that the differences in ancillary ligands, leads to dramatically different reactivity. The nitride group, in nitride-bridged cationic and anionic diuranium(IV) complexes supported by –N(SiMe<sub>3</sub>)<sub>2</sub> ligands, is resistant toward protonation by weak acids, while stronger acids result in ligand loss by protonolysis. Moreover, the basic –N(SiMe<sub>3</sub>)<sub>2</sub> ligands promote the N–H heterolytic bond cleavage of NH<sub>3</sub>, yielding a “naked” diuranium complex containing three bridging ligands, a nitride (N<sup>3–</sup>) and two NH<sub>2</sub> ligands. Conversely, in the nitride-bridged diuranium(IV) complex supported by –OSi(O<sup>t</sup>Bu)<sub>3</sub> ligands, the nitride group is easily protonated to afford NH<sub>3</sub>, which binds the U(IV) ion strongly, resulting in a mononuclear U–NH<sub>3</sub> complex, where NH<sub>3</sub> can be displaced by addition of strong acids. Furthermore, the U–OSi(O<sup>t</sup>Bu)<sub>3</sub> bonds were found to be stable, even in the presence of stronger acids, such as NH<sub>4</sub>BPh<sub>4</sub>, therefore indicating that –OSi(O<sup>t</sup>Bu)<sub>3</sub> supporting ligands are well suited to be used when acidic conditions are required, such as in the H<sup>+</sup>/e<sup>–</sup> mediated catalytic conversion of N<sub>2</sub> to NH<sub>3</sub>.

## Introduction

Uranium nitrides were identified more than 100 years ago as active catalysts in the conversion of dinitrogen (N<sub>2</sub>) to ammonia (NH<sub>3</sub>),<sup>1</sup> and very recently, the stoichiometric conversion of N<sub>2</sub> into NH<sub>3</sub> by molecular uranium complexes was reported.<sup>2</sup> Notably, dinuclear uranium(III) complexes<sup>2a,3</sup> or dinuclear U(IV) complexes combined with an external reducing agent,<sup>2b</sup> were capable of carrying out the four electron reduction of N<sub>2</sub>. Full cleavage of N<sub>2</sub> to nitrides has also been reported,<sup>2c,4a,b</sup> where the resulting hydrazido and nitride ligands could be further reduced and protonated, yielding stoichiometric amounts of NH<sub>3</sub>.<sup>2,4b</sup>

The conversion of metal nitrides to NH<sub>3</sub> is an essential step in dinitrogen fixation, where effective nitride protonation is crucial in building catalytic cycles.<sup>5</sup> A key challenge in developing catalytic N<sub>2</sub> reduction to NH<sub>3</sub>, is the simultaneous addition of reducing agent and acid (H<sup>+</sup>), while maintaining the structure of the catalyst, by avoiding ligand protonation and irreversible binding of NH<sub>3</sub>. However, studies addressing the reactivity of nitrides with protonating agents<sup>6</sup> are limited to d-block metals, with few instances of imido (NH<sup>2–</sup>), amido

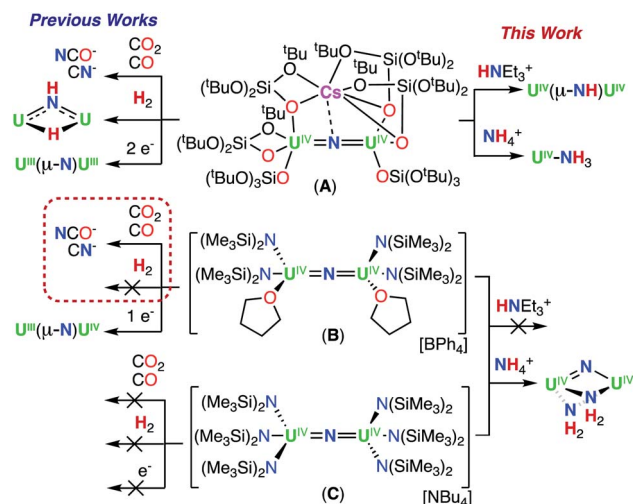
(NH<sub>2</sub><sup>–</sup>), and ammonia (NH<sub>3</sub>) bound products being isolated and characterized. Protonation of the ligand<sup>7</sup> or the metal center,<sup>8</sup> rather than the nitride, is common, and favoring protonation of the nitride can be challenging. The irreversible binding of NH<sub>3</sub>, or its reactivity with the metal complex, may also constitute an important disadvantage in catalyst design. Despite the inherent stability of the N–H bonds in NH<sub>3</sub>, activation under mild conditions can occur through ligand–metal cooperation,<sup>9</sup> where the presence of basic ligands can result in the redox-neutral heterolysis of NH<sub>3</sub> and subsequent ligand protonolysis. Facile N–H activation of NH<sub>3</sub> *via* metal–ligand cooperative addition was also reported in one instance for a uranium complex.<sup>10</sup>

Since the first examples of uranium nitrides were isolated in the gas phase<sup>11</sup> and in solution,<sup>4a,12</sup> uranium nitride complexes have been the subject of an increasing number of reports. Mononuclear, dinuclear, polynuclear, mono- and bis-nitride complexes that contain uranium in oxidation states ranging from (III) to (VI) have been synthesized.<sup>13</sup> Several systems have revealed high reactivity towards small molecules, such as CO<sub>2</sub>, CO, H<sub>2</sub>, and N<sub>2</sub>,<sup>2a,b,3,13f,i,k,14a–q</sup> and demonstrated their ability to promote C–H bond activation.<sup>13m,15a–d</sup> Moreover, addition of excess strong acid to terminal or bridging uranium nitrides, derived from azide or N<sub>2</sub>, has been reported to yield variable amounts of ammonia (20–100%).<sup>2c,4b,13i,l,14o,q</sup> However, the isolation and characterization of partially protonated, intermediate species have not been reported thus far. Additionally, the site of first protonation, the parameters controlling the yield, or the fate of the uranium complex have not yet been elucidated.

Institut des Sciences et Ingénierie Chimiques, École Polytechnique Fédérale de Lausanne (EPFL), 1015 Lausanne, Switzerland. E-mail: marinella.mazzanti@epfl.ch

† Electronic supplementary information (ESI) available: Synthetic methods, NMR spectra, crystallographic data. CCDC 2097071, 2097072 and 2097366–2097369. For ESI and crystallographic data in CIF or other electronic format see DOI: 10.1039/d1sc03957a





Scheme 1 Previously reported dinuclear  $U^{IV}$ -nitride complexes **A**, **B**, and **C** and their previous and currently described reactivity.

We reasoned that investigating the protonation of uranium-nitrides, supported by different ancillary ligands, and their interaction with the resulting  $NH_3$ , could provide insight into the parameters controlling the reactivity. This would allow us to harness significant elements for the design of complexes active in the  $H^+/e^-$  mediated catalytic conversion of  $N_2$  to  $NH_3$ .

We have previously reported that  $-OSi(O^tBu)_3$  are versatile ancillary ligands for the synthesis of bridging and terminal uranium nitrides in oxidation states ranging from (III) to (VI).<sup>13g,i,l,14g,16</sup> Moreover, they have allowed the isolation of nitride and oxide bridged diuranium(III) complexes which promote the stoichiometric conversion of  $N_2$  to  $NH_3$ .<sup>2a,3,4b</sup> We also found that using  $-OSi(O^tBu)_3$  (complex **A**; Scheme 1)<sup>14h,i,l</sup>

versus  $-N(SiMe_3)_2$  (**B** and **C**)<sup>13k,m,17,18</sup> as supporting ligands leads to significant differences in reactivity of analogous nitride and oxide bridged diuranium complexes with respect to reducing agents ( $KC_8$ ), electrophilic molecules such as  $CO_2$ ,  $CO$ , and  $H_2$  (Scheme 1), and  $N_2$  reduction.<sup>2a,18</sup>

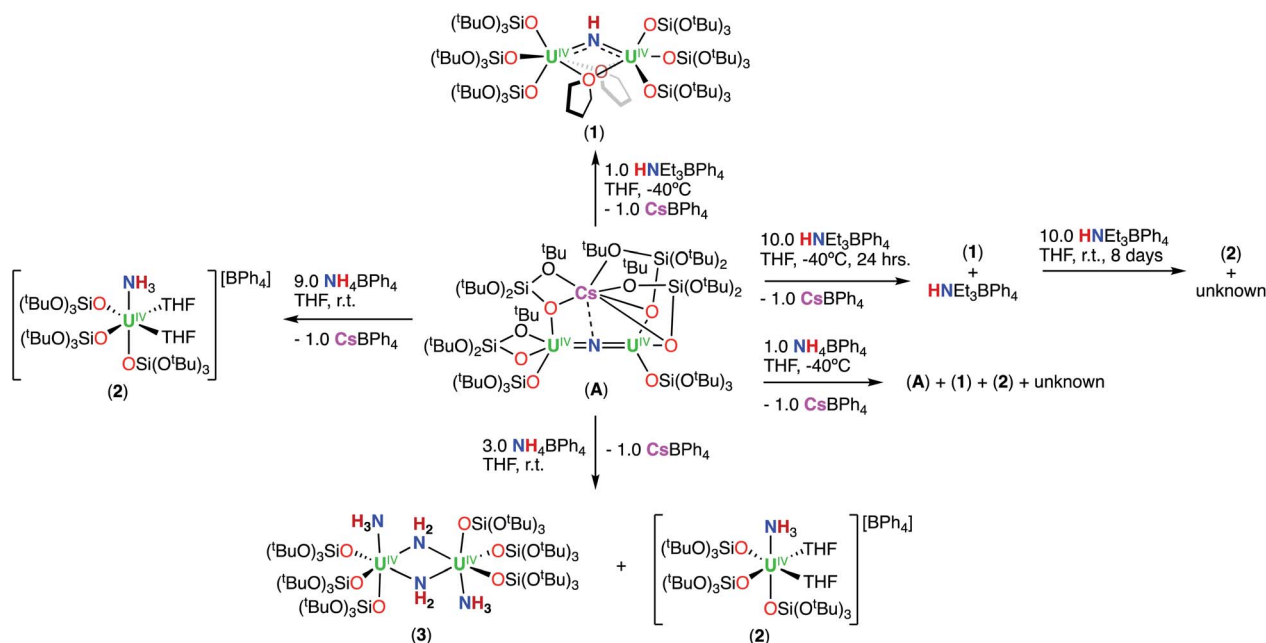
Herein, we report the comparative studies for the reactions of  $H^+$  and  $NH_3$  with the diuranium(IV) bridging nitrides, **A**, **B** and **C**. We show that the different ancillary ligands lead to dramatically different reactivity, resulting in the isolation of a stable terminal  $NH_3$  complex (**2**) and a “naked” diuranium complex containing three bridging ligands, a nitride ( $N^{3-}$ ) and two  $NH_2$  ligands, providing important information on the species that can be formed during conversion of nitride to ammonia.

## Results and discussion

### Reactivity of $OSi(O^tBu)_3$ -containing complexes

First, we were interested in probing the reactivity of the previously reported anionic bridging nitride (**A**), supported by  $-OSi(O^tBu)_3$  ligands. The nitride link in this complex has been described to be more reactive towards electrophiles than in the analogous  $-N(SiMe_3)_2$  complex **C** (Scheme 1) but its reactivity with acids was not investigated.<sup>13k</sup>

Addition of 1.0 equiv. of  $NH_4BPh_4$  to a solution of **A** in  $d_8$ -THF at  $-40^\circ C$  resulted in the partial consumption of **A** and appearance of new resonances in the  $^1H$  NMR spectrum (Fig. S1<sup>†</sup>). While some resonances remain unidentified, two sets of resonances were assigned to the complexes  $[(U^{IV}(OSi(O^tBu)_3)_3(THF))_2(\mu-NH)]$  (**1**), which could be cleanly produced using the weaker acid,  $HNEt_3BPh_4$  (Scheme 2 and the following section), and  $[U^{IV}(OSi(O^tBu)_3)_3(THF)_2(NH_3)][BPh_4]$  (**2**; see below).



Scheme 2 Reactivity of complex **A** toward various  $H^+$  (acid) sources.



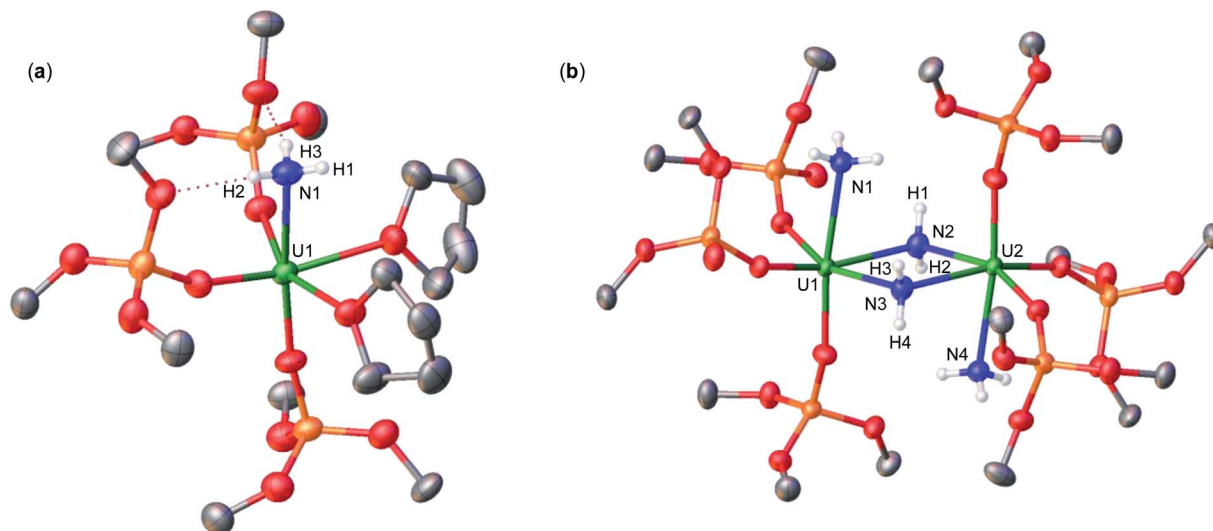


Fig. 1 Molecular structures of (a)  $[\text{U}^{\text{IV}}(\text{OSi}(\text{O}^t\text{Bu})_3)_3(\text{THF})_2(\text{NH}_3)][\text{BPh}_4]$ , **2**, and (b)  $[(\text{U}^{\text{IV}}(\text{OSi}(\text{O}^t\text{Bu})_3)_3(\text{NH}_3)_2)(\mu\text{-NH}_2)_2]$ , **3**, with thermal ellipsoids drawn at the 50% probability level. Hydrogen atoms on the  $-\text{OSi}(\text{O}^t\text{Bu})_3$  ligands, methyl groups, and the  $\text{BPh}_4$  anion in (a) have been omitted for clarity.

Addition of 3.0 equiv. of  $\text{NH}_4\text{BPh}_4$  to a solution of **A** in  $d_8$ -THF resulted in immediate formation of a teal solution and precipitation of a white solid. Crystals of two products were isolated at  $-40^\circ\text{C}$  from a concentrated  $\text{Et}_2\text{O}$  solution of the reaction mixture and characterized by XRD analysis as the complexes  $[\text{U}^{\text{IV}}(\text{OSi}(\text{O}^t\text{Bu})_3)_3(\text{THF})_2(\text{NH}_3)][\text{BPh}_4]$  (**2**) (Fig. 1a), and  $[(\text{U}^{\text{IV}}(\text{OSi}(\text{O}^t\text{Bu})_3)_3(\text{NH}_3)_2)(\mu\text{-NH}_2)_2]$  (**3**) (Fig. 1b). Analysis by  $^1\text{H}$  NMR spectroscopy of the reaction mixture was consistent with the formation of complexes **2** and **3** in a 1.1 : 1 ratio (Fig. S2†). Few pure crystals of **3** could be obtained for  $^1\text{H}$  NMR spectroscopy, but attempts to isolate larger quantities of pure material remained unsuccessful, resulting in mixtures of both **2** and **3**. The  $^1\text{H}$  NMR spectrum of complex **3** in  $d_8$ -THF displays two signals at  $\delta$  5.1 and  $-5.6$  ppm, corresponding to the  $-\text{OSi}(\text{O}^t\text{Bu})_3$  ancillary ligands, and two resonances at  $-10.7$  and  $-70.6$  ppm assigned to the amido ( $\text{NH}_2^-$ ) and  $\text{NH}_3$  resonances, respectively.

Addition of excess (9.0 equiv.)  $\text{NH}_4\text{BPh}_4$  to a solution of **A** in  $d_8$ -THF, resulted in a pale blue mixture. After 12 hours, the  $^1\text{H}$  NMR spectrum of this mixture shows only the presence of the signals assigned to complex **2** (Fig. S4†). Large plate, teal crystals suitable for XRD analysis of  $[\text{U}^{\text{IV}}(\text{OSi}(\text{O}^t\text{Bu})_3)_3(\text{THF})_2(\text{NH}_3)][\text{BPh}_4]$  (**2**), were obtained from a concentrated  $\text{Et}_2\text{O}$  solution at  $-40^\circ\text{C}$  (Fig. 1b and Scheme 2), in 82% yield. The  $^1\text{H}$  NMR spectrum of complex **2** in  $d_8$ -THF displays three aromatic  $\text{BPh}_4$  phenyl signals and one broad resonance at  $\delta$  9.6 ppm, corresponding to the  $-\text{OSi}(\text{O}^t\text{Bu})_3$  ancillary ligands. The resonance at  $-160.1$  ppm is assigned to the uranium bound  $\text{NH}_3$ .

The clean formation of **2**, from the reaction of **A** with excess  $\text{NH}_4\text{BPh}_4$  and its isolation in 82% yield, cannot be explained only by the protonation of the nitride, but requires binding of  $\text{NH}_3$  released during protonation by  $\text{NH}_4\text{BPh}_4$ . In order to confirm that the  $\text{NH}_3$  ligand in **2**, arises both from nitride protonation and from added  $\text{NH}_4\text{BPh}_4$ , we performed the reaction of **A** with isotopically enriched  $^{15}\text{NH}_4\text{BPh}_4$  to yield **2**- $^{14/15}\text{N}$ .

Adding a solution of  $\text{HCl}$  in  $\text{Et}_2\text{O}$  to **2**- $^{14/15}\text{N}$  leads to the formation of both  $^{15}\text{NH}_4\text{Cl}$  and  $^{14}\text{NH}_4\text{Cl}$  (97% total yield), indicated by a doublet and triplet respectively in the  $^1\text{H}$  NMR spectrum. The ratio of  $^{15}\text{NH}_4\text{Cl} : ^{14}\text{NH}_4\text{Cl}$  is quite large (8 : 1 ratio), because of the large excess (9.0 equiv.) of  $^{15}\text{NH}_4\text{BPh}_4$  used in the initial synthesis of **A**  $\rightarrow$  **2**- $^{14/15}\text{N}$ . The  $\text{NH}_3$  ligand in **2** binds quite strongly to the  $\text{U}(\text{IV})$  center, as it could not be removed under dynamic vacuum for a few hours, but is removed upon addition of strong acids.

The isolation of complex **3**, when 3.0 equiv. of  $\text{NH}_4\text{BPh}_4$  are added to **A**, suggests that the formation of **2** proceeds through the bis-amido intermediate **3**, which can be further protonated to yield the mononuclear terminal  $\text{NH}_3$  complex. We suggest that the formation of the bis-amido intermediate **3**, involves a putative mono-amido complex,  $[(\text{U}^{\text{IV}}(\text{OSi}(\text{O}^t\text{Bu})_3)_3(\text{NH}_3)_2)(\mu\text{-NH}_2)][\text{BPh}_4]$  (**3<sub>int</sub>**) that undergoes ligand disproportionation to yield **2** and **3** (Scheme S1†).

In order to isolate intermediates with a lower degree of protonation, we investigated the reaction of **A** with  $\text{HNET}_3\text{BPh}_4$ , a weaker acid compared to  $\text{NH}_4\text{BPh}_4$ . Addition of 1.0 equiv. of  $\text{HNET}_3\text{BPh}_4$  to a solution of **A** in  $d_8$ -THF at  $-40^\circ\text{C}$  resulted in a green solution and precipitation of a white solid ( $\text{CsBPh}_4$ ). The  $^1\text{H}$  NMR spectrum of the reaction mixture reveals the complete consumption of **A** and the clean formation of a new species (Fig. S5†). Pale green crystals of  $[(\text{U}^{\text{IV}}(\text{OSi}(\text{O}^t\text{Bu})_3)_3)_2(\mu\text{-THF})_2(\mu\text{-NH})]$  (**1**) were obtained in 69% yield from a concentrated THF solution at  $-40^\circ\text{C}$  (Scheme 2 and Fig. 2). The  $^1\text{H}$  NMR spectrum of complex **1** in  $d_8$ -THF displays a broad resonance at  $\delta$  0.72, corresponding to the  $-\text{OSi}(\text{O}^t\text{Bu})_3$  ancillary ligands, and another broad resonance at  $\delta$  150.3 ppm assigned to the imido ( $\text{NH}^{2-}$ ) group. A similar chemical shift (176.5 ppm) was observed for the imido group in the previously reported bis-imido bridged complex  $[\text{K}_2\{[\text{U}(\text{OSi}(\text{O}^t\text{Bu})_3)_3]_2(\mu\text{-NH})_2\}]$ .<sup>13i</sup>

We also investigated the addition of excess  $\text{HNET}_3\text{BPh}_4$  to **A**, in order to determine if protonation of the imido ( $\text{NH}^{2-}$ ) group



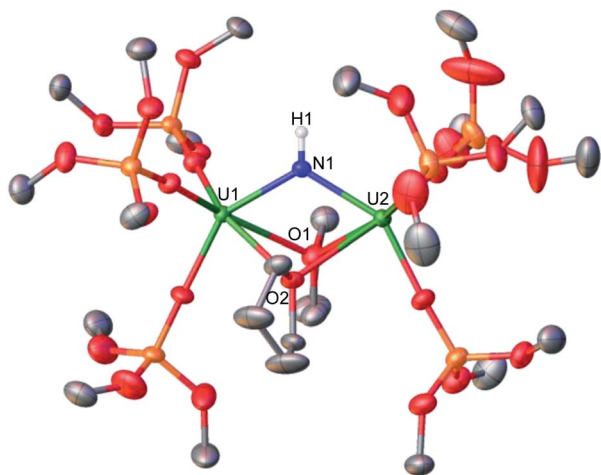


Fig. 2 Molecular structure of  $[(U^{IV}(OSi(O^tBu)_3)_3)_2(\mu-NH)(\mu-NH)] [BPh_4]$ , **1**, with thermal ellipsoids drawn at the 50% probability level. Hydrogen atoms and methyl groups on the  $-OSi(O^tBu)_3$  ligands have been omitted for clarity.

in **1**, would yield the  $NH_3$  complex, **2**. Addition of excess (10 equiv.)  $HNEt_3BPh_4$  to a solution of **A** in  $d_8$ -THF at  $-40^\circ C$  resulted in the formation of a pale green solution with precipitation of a white solid ( $CsBPh_4$ ) (Scheme 2). The reaction mixture was brought to room temperature and analysis by  $^1H$  NMR spectroscopy revealed resonances consistent with the presence of **1** and unreacted  $HNEt_3BPh_4$ . Further stirring of the solution for an additional 2 days at room temperature resulted in a blue solution, with partial consumption of **1**. After 8 days,  $^1H$  NMR spectroscopy indicated the complete consumption of **1** with appearance of the resonance at  $\delta$  9.6 ppm, assigned to the  $NH_3$  complex (**2**) in 40% yield, together with unidentified signals (Fig. S6a-d $\dagger$ ). The absence of the resonance at  $\delta$   $-160.1$  ppm, assigned to the uranium bound  $NH_3$ , is attributed to the fast exchange of the  $NH_3$  ligand in the presence of excess  $HNEt_3BPh_4$ . We were able to confirm this by addition of 10.0 equiv.  $HNEt_3BPh_4$  to a solution of **2** in  $d_8$ -THF. Over 12 hours, we see that the signal corresponding to the uranium bound  $NH_3$  disappears (Fig. S7 $\dagger$ ). These results indicate that **1** is further protonated to the  $-NH_3$  containing species by excess  $HNEt_3BPh_4$ , but requires longer reaction times to yield **2**. The formation of **2** (40% yield) in this reaction arises from cleavage

of the  $U=N=U$  bridge, which requires the formation of other U-containing products that we were unable to identify.

### Structural characterization of $OSi(O^tBu)_3$ -containing complexes

The solid-state molecular structures of complexes **1**, **2**, and **3** were determined by X-ray diffraction studies. The metrical parameters are presented in Table 1, including those previously reported for complex **A**.

Complex **1** crystallizes in the space group  $C2/c$  with one molecule per asymmetric unit. The solid-state molecular structure of **1** shows the presence of a neutral diuranium(IV) complex where each uranium is bound by three  $-OSi(O^tBu)_3$  ancillary ligands and are bridged by an imido ( $NH^2-$ ) ligand and two THF molecules (Fig. 2). The U–N–U bond angle changes dramatically from linear in **A** (U–N–U:  $170.2(3)^\circ$ ) to bent in **1** ( $118.3(3)^\circ$ ). The U–N bond distances in **1** are elongated (U1–N1:  $2.243(7)$ , U2–N1:  $2.219(6)$  Å) in comparison to **A**, consistent with a bridging imido ( $\mu-NH$ ).<sup>14f</sup>

Complex **2** crystallizes in the space group  $P\bar{1}$  with one molecule per asymmetric unit. Its solid-state molecular structure shows the presence of an ion pair consisting of one  $BPh_4^-$  anion and the  $[U^{IV}(OSi(O^tBu)_3)_3(THF)_2(NH_3)]$  cation comprising of a terminal  $U^{IV}-NH_3$  bound ligand (Fig. 1a). Only two examples of crystallographically characterized U– $NH_3$  complexes have been reported so far: the bis(1,1,1,5,5,5-hexafluoropentane-2,4-dionato) $NH_3$ -uranyl(vi)<sup>19</sup> and a series of trinuclear complexes of formula  $[(NH_3)_8U(\mu-N)(NH_3)_3(X)_2U(\mu-N)U(NH_3)_8]Y_n \cdot ZNH_3$  ( $X = NH_3, Br^-,$  or  $Cl^-$ ;  $n = 6-8$ ;  $Y = Cl^-$  or  $Br^-$ ;  $Z = 26, 21,$  or  $6$ ).<sup>20</sup> Where the U– $NH_3$  bond distances in these examples,  $2.48(6)$ <sup>19</sup> and  $2.605(3)$ <sup>20</sup> respectively, are consistent with the U1–N1 ( $2.540(4)$  Å) bond distance in complex **2**. Additionally, the U– $NH_3$  bond distance in **2** is dramatically elongated in comparison to previously reported terminal amido ( $NH_2$ ) complexes,  $[U(1,2,4-(^tBu)_3C_5H_2)_2(NH_2)_2]$  (U– $N_{amido}$ ;  $2.228(4)$  Å),  $[U(Tren^{TIPS})(NH_2)]$  (U– $N_{amido}$ ;  $2.194(5)$  Å),<sup>21</sup> and  $[U(COT^{TIPS2})(Cp^*)(NH_2)]$  (U– $N_{amido}$ ;  $2.217(4)$  Å),<sup>10</sup> further supporting a terminal bound  $NH_3$  molecule. The protons of the  $NH_3$  ligand can be crystallographically identified, making their assignment unambiguous.

Complex **3** crystallizes in the space group  $P\bar{1}$  with 0.5 molecules per asymmetric unit. Its solid-state molecular structure

Table 1 Selected bond lengths (Å) and angles ( $^\circ$ ) of the previously reported complexes  $[Cs(U^{IV}(OSi(O^tBu)_3)_3)_2(\mu-N)]$ , **A**, and  $[(U^{IV}(N(SiMe_3)_2)(THF)_2)(\mu-N)] [BPh_4]$ , **B**, as well as complexes  $[(U^{IV}(OSi(O^tBu)_3)_3)_2(\mu-NH)]$ , **1**,  $[(U^{IV}(OSi(O^tBu)_3)_3(THF)_2)(NH_3)] [BPh_4]$ , **2**,  $[(U^{IV}(OSi(O^tBu)_3)_3)(NH_3)_2(\mu-NH_2)_2]$ , **3**,  $[(U^{IV}(N(SiMe_3)_2)(THF)_3)_2(\mu-NH)_2] [BPh_4]$ , **4**, and  $[(U^{IV}(THF)_4)_2(\mu-N)(\mu-NH_2)_2] [BPh_4]$ , **5**

Complex	<b>A</b> (ref. 14h)	<b>1</b>	<b>2</b>	<b>3</b>	<b>B</b> (ref. 13k)	<b>4</b>	<b>5</b>
U– $N_{nitride}$	2.058(5)	—	—	—	2.055(3)	—	2.062(3); 2.018(3)
U– $N_{imido}$	—	NH: 2.243(7); 2.219(6)	—	—	—	NH: 2.179(5); 2.198(6)	—
U– $N_{amido}$	—	—	$NH_3$ : 2.540(4)	$NH_3$ : 2.608(3) $NH_2$ : 2.451(3); 2.463(2)	—	—	$NH_2$ : 2.449(3); 2.455(3)
U–N–U	170.2(3)	—	—	—	168.97(14)	—	107.41(12)
U–NH–U	—	118.3(3)	—	—	—	106.6(2)	—
U– $NH_2$ –U	—	—	—	106.5(1)	—	—	84.36(9)



can be described as a neutral complex consisting of a dinuclear  $U^{IV}/U^{IV}$  core, comprising of two  $[U^{IV}(OSi(O^tBu)_3)_3(NH_3)]$  units bridged by two amido ( $NH_2^{1-}$ ) ligands (Fig. 1b). The U1–N1 and U2–N4 (2.608(3) Å) bond distances are consistent with a terminal  $NH_3$ , as found in **2** (U1–N1: 2.540(4) Å). The U1–N2 = 2.451(3) Å and U1–N3 = 2.463(2) Å bond distances are consistent with two bridging amido ( $NH_2^{1-}$ ) ligands,<sup>14q</sup> with delocalized charge on the uranium ions as indicated by the nearly symmetrical U– $N_{amido}$  metrical parameters. The protons of the imido ligands can be crystallographically identified, making their assignment unambiguous.

Next, we investigated protonation of the previously reported dinuclear  $U^{IV}$ -nitride complexes bearing more basic  $-N(SiMe_3)_2$  ancillary ligands.

### Reactivity of $N(SiMe_3)_2$ -containing complexes

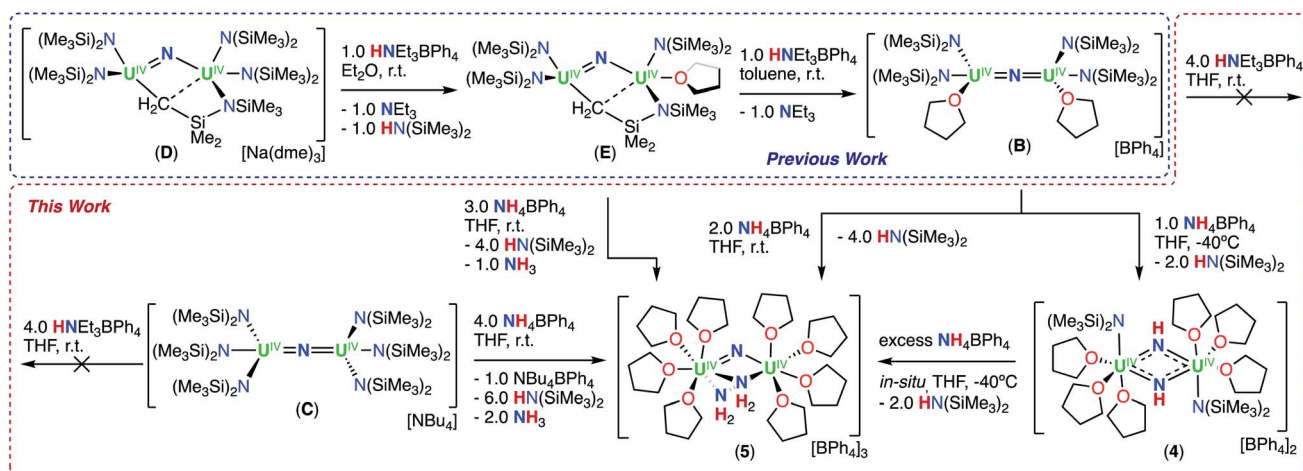
First, we probed the reactivity of complex, **B** with  $CO_2$ ,  $CO$ , and  $H_2$  to compare it with that of complexes **A** and **C** (Scheme 1). Previous work has shown that **B** has an increased reactivity toward reducing agents in comparison to the all  $-N(SiMe_3)_2$ , complex **C**, but the reactivity with  $CO_2$ ,  $CO$ , and  $H_2$  was not explored in the previous report.<sup>13m</sup> We found that complex **B** reacts with 2.0 equiv. of  $^{13}CO_2$  in  $d_8$ -THF over 4 days, in which **B** is fully consumed and results in a complicated  $^1H$  NMR spectrum (Fig. S11†). Attempts to grow single crystals from the reaction mixture were unsuccessful. However, after the removal of volatiles and hydrolysis with  $D_2O$  (pD = 12) of the reaction residue,  $N^{13}CO^-$  was identified by  $^{13}C$  NMR spectroscopy (Fig. S12†), similarly to what observed for complex **A**.

Complex **B** reacts with 2.0 equiv. of  $^{13}CO$  in  $d_8$ -THF over 6 days, in which **B** is fully consumed and results in a complicated  $^1H$  NMR spectrum (Fig. S13†). Attempts to grow crystals from the reaction mixture were unsuccessful. However, after quenching the reaction mixture with  $D_2O$  (pD = 12),  $^{13}CN^-$  was identified by  $^{13}C$  NMR spectroscopy (Fig. S14†). This indicates that, as previously reported for **A**, which reacts readily with  $CO$  to yield  $[Cs(U(OSi(O^tBu)_3)_3)_2(\mu-CN)(\mu-O)]$ ,<sup>14i</sup> the nucleophilic character of the bridging nitride promotes the cleavage and deoxygenation of

$CO$  to afford a  $C\equiv N$  triple bond and a bridging oxo. Conversely, the all  $-N(SiMe_3)_2$ , complex **C**, has been previously shown to be unreactive in the presence of stoichiometric and excess quantities of  $CO$ .<sup>13k</sup> These results suggest an increased nucleophilicity of the nitride in the cationic complex **B**, compared to the anionic complex **C**. However, complex **B** does not react with  $H_2$  similarly to what was found for complex **A** (Fig. S15†). The lack of reactivity with  $H_2$  indicates a decreased nucleophilicity of the nitride in **B** compared to **A**, which was found to activate  $H_2$  yielding the first example of a bridging imido-hydride complex,  $[Cs(U(OSi(O^tBu)_3)_3)_2(\mu-NH)(\mu-H)]$ .<sup>14j</sup> Therefore, we became interested in how these differences in reactivity would extend to the reaction with acids ( $HNEt_3BPh_4$  and  $NH_4BPh_4$ ).

Next, we probed the reactivity of cationic bridging nitride (**B**), which was synthesized as reported by our group<sup>13m</sup> by successive protonolysis of one  $-N(SiMe_3)_2$  ligand in the complex **D**, previously reported by Fortier and Hayton,<sup>13b</sup> and of the metal-amide methanide bond in **E**, using a total of 2.0 equiv. of  $HNEt_3BPh_4$  (Scheme 3). Addition of excess (4.0 equiv.)  $HNEt_3BPh_4$  to a solution of **B** in  $d_8$ -THF, resulted in unreacted starting materials as seen by  $^1H$  NMR spectroscopy (Fig. S16†). Therefore, we pursued the protonation using the stronger acid,  $NH_4BPh_4$ , resulting in different reactivity compared to what was found for the  $-OSi(O^tBu)_3$  complex, **A**.

$^1H$  NMR studies showed that addition of 1.0 equiv. of  $NH_4BPh_4$  to a solution of **B** in  $d_8$ -THF resulted in the formation of a new species displaying a resonance at  $\delta$  12.6 ppm and unreacted **B** (Fig. S17†). Golden crystals suitable for XRD analysis were obtained from the reaction mixture at  $-40^\circ C$  after 12 hours. The solid-state molecular structure shows the presence of a dinuclear  $U^{IV}/U^{IV}$  bridging bis-imido ( $NH_2^{2-}$ ) complex,  $[(U^{IV}(N(SiMe_3)_2)(THF)_3)_2(\mu-NH)_2][BPh_4]_2$  (**4**) (Fig. 3a and Scheme 3). The product is insoluble in most common solvents including toluene,  $Et_2O$ , THF, and  $n$ -hexanes, but is soluble in pyridine. The  $^1H$  NMR spectrum of the isolated crystals of **4** in  $d_5$ -pyridine, displays a resonance at  $\delta$  13.2 ppm, three aromatic  $BPh_4$  phenyl signals, and THF resonances due to the displacement



Scheme 3 Reactivity of complexes **B**, **C**, **D**, and **E** toward various  $H^+$  (acid) sources.



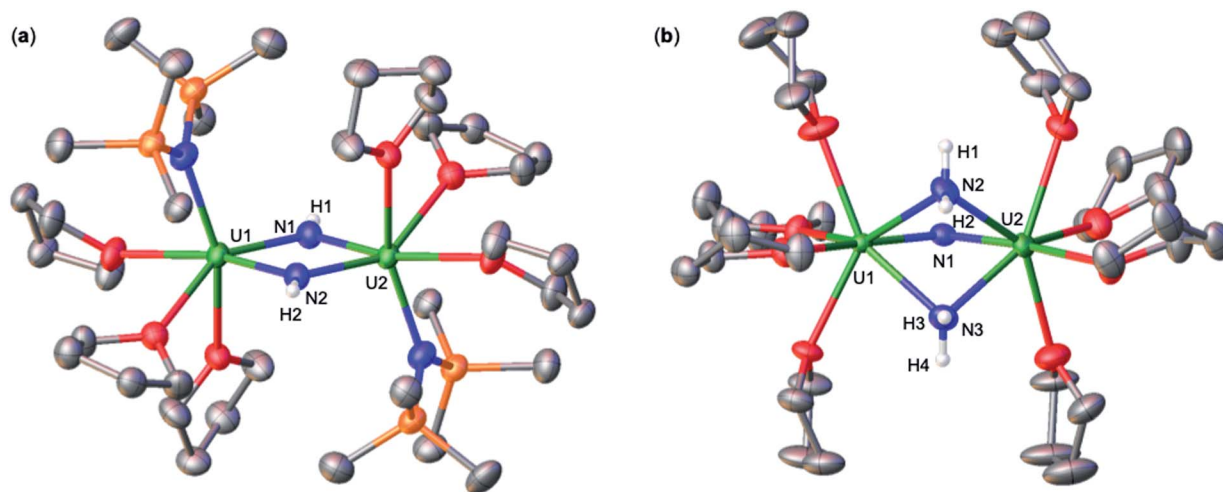


Fig. 3 Molecular structures of (a)  $[(U^{IV}(N(SiMe_3)_2)(THF)_3)_2(\mu-NH_2)] [BPh_4]_2$ , **4**, and (b)  $[(U^{IV}(THF)_4)_2(\mu-N)(\mu-NH_2)_2] [BPh_4]_3$ , **5**, with thermal ellipsoids drawn at the 50% probability level. Hydrogen atoms and methyl groups on the ancillary ligands, and  $BPh_4$  counterions have been omitted for clarity.

upon coordination of  $d_5$ -pyridine, but were unable to identify resonances for the imido ( $NH_2^-$ ) groups (Fig. S18<sup>†</sup>).

Attempts to isolate **4** analytically pure failed most likely due to the cocrystallization of **B**. Recrystallization of a pyridine solution containing **4**, by slow diffusion of  $Et_2O$  at  $-40^\circ C$ , resulted in single crystals suitable for XRD analysis, identifiable as the pyridine adduct of **4**,  $[(U^{IV}(N(SiMe_3)_2)(pyridine)_3)_2(\mu-NH_2)] [BPh_4]_2$  (**4-pyr**; Fig. S24<sup>†</sup>). All metrical parameters are analogous to the THF adduct of **4**. Attempts to isolate larger quantities of **4-pyr** proved to be unsuccessful.

$^1H$  NMR studies showed that addition of 2.0 equiv.  $NH_4BPh_4$  to **B** in  $d_8$ -THF after 20 minutes, results in the partial disappearance of the signals of **B**, and in the appearance of the resonance at  $\delta$  12.6 ppm assigned to **4**. The  $^1H$  NMR spectrum of the reaction mixture measured after 12 hours showed complete disappearance of the signals corresponding to **B** and to **4**, with concomitant appearance of the resonance assigned to  $HN(SiMe_3)_2$  (Fig. S19a and b<sup>†</sup>). Furthermore, the reaction mixture, after standing 12 hours at  $-40^\circ C$ , afforded gold crystals of  $[(U^{IV}(THF)_4)_2(\mu-N)(\mu-NH_2)_2] [BPh_4]_3$  (**5**) in 83% yield (Fig. 3b and Scheme 3). The product is insoluble in most common solvents including toluene,  $Et_2O$ , THF, and  $n$ -hexanes, but is soluble in pyridine. The  $^1H$  NMR spectrum of complex **5** in  $d_5$ -pyridine displays three aromatic  $BPh_4$  phenyl signals, THF resonances due to the displacement upon coordination of  $d_5$ -pyridine, and two amido ( $NH_2^-$ ) resonances at  $-468$  ppm. Additionally, complex **5** can also be obtained in 89% yield through direct addition of 3.0 equiv.  $NH_4BPh_4$  to complex **E**. Therefore, isolating complex **B** is not required for the synthesis of complex **5** (Scheme 3).

The presence of two amido ( $NH_2^-$ ) bridging groups in **5**, can be interpreted in terms of the binding and concomitant N-H cleavage of two  $NH_3$  molecules. This involves protonation of the  $U^{IV}-N(SiMe_3)_2$  bonds, resulting in the release of four molecules of  $HN(SiMe_3)_2$ . To date, there is only one other example of the facile N-H activation of  $NH_3$  by an uranium complex. The  $U^{IV}$

“tucked-in” mixed-sandwich complex,  $[U(\eta^5-COT^{TIPS2})(\eta^5-\kappa^1-C_5Me_4CH_2)]$ , was reported to promote the ligand assisted  $NH_3$  activation yielding the terminal  $U^{IV}-NH_2$  complex  $[U(COT^{TIPS2})Cp^*(NH_2)]$ .<sup>22</sup> Uranium complexes of primary amides remain rare,<sup>21</sup> and complex **5** provides the second example of a bridging amide.<sup>13a</sup>

In order to confirm that the two bridging amido ( $NH_2^-$ ) moieties in **5**, are derived from  $NH_3$ , we prepared the  $^{15}N$  labeled analogue **5- $^{14/15}N$**  by reacting the isotopically enriched  $^{15}NH_4BPh_4$  with **B**. Adding a solution of HCl in  $Et_2O$  to **5- $^{14/15}N$**  leads to the formation of both  $^{15}NH_4Cl$  and  $^{14}NH_4Cl$  (95% yield), indicated by a doublet and triplet respectively in the  $^1H$  NMR spectrum (2 : 1 ratio,  $^{15}NH_4Cl$  :  $^{14}NH_4Cl$ ).

These results indicate that formation of the bridging nitride bis-amido complex (**5**) occurs *via* protonation of two  $-N(SiMe_3)_2$  ligands, binding of the resulting  $NH_3$ , and subsequent N-H heterolysis of  $NH_3$  assisted by the remaining two basic  $-N(SiMe_3)_2$  ligands. We suggest that the reaction proceeds first through the imido ( $NH_2^-$ ) intermediate (**4**), which arises from protonation of one  $U^{IV}-N(SiMe_3)_2$  bond and N-H heterolysis of one  $NH_3$  molecule with concomitant elimination of two  $HN(SiMe_3)_2$  ligands. This is likely to occur *via* a nitride-amido bridged complex,  $[(U^{IV}(N(SiMe_3)_2)(THF))_2(\mu-NH_2)(\mu-N)] [BPh_4]_2$  (**4<sub>int</sub>**) but the higher nucleophilicity of the nitride, compared to **B**, results in a proton redistribution, yielding complex **4** (Scheme S2<sup>†</sup>). Further protonation of a  $U^{IV}-N(SiMe_3)_2$  bond in **4**, followed by  $NH_3$  binding and N-H heterolysis, should afford a bis-imido, mono-amido complex,  $[(U^{IV}(THF)_4)_2(\mu-NH_2)(\mu-NH_2)] [BPh_4]_3$  (**5<sub>int</sub>**), but subsequent rearrangement of the protons instead yields complex **5**. Such redistribution of protons can be explained in terms of an increased stability of the nitride compared to the imide when two  $N(SiMe_3)_2$  ligands are replaced by two THF and one amido ligands. Previous studies demonstrated the important effect of ancillary ligands on the stability and reactivity of bridging uranium nitrides.<sup>13k</sup>



Next, we probed the protonation and reactivity of the neutral nitride complex, **C**. Complex **C** is analogous to **B** in that it contains  $-\text{N}(\text{SiMe}_3)_3$  ancillary ligands, but has two additional ligands within the complex. Previous studies from our group showed that **C** is less reactive towards small molecule activation in comparison to complexes **B** and **A** (Scheme 1). This was interpreted, based on DFT studies, in terms of a decreased nucleophilicity of the nitride moiety, due to an increased bond order of the bridging nitride in the  $\text{U}^{\text{IV}}-\text{N}(\text{SiMe}_3)_3$  complex **C** compared to the  $\text{U}^{\text{IV}}-\text{OSi}(\text{O}^t\text{Bu})_3$  complex **A**.<sup>13k</sup> Therefore, we investigated if protonation of the amide ligands and  $\text{NH}_3$  activation could also occur in complex **C**.

Similar to the reactivity of **B** with  $\text{HNET}_3\text{BPh}_4$ , addition of 4.0 equiv. of  $\text{HNET}_3\text{BPh}_4$  to a solution of **C** in  $d_8$ -THF resulted in no reaction (Fig. S20†). Alternatively, treatment with 3.0 equiv.  $\text{NH}_4\text{BPh}_4$  resulted in an immediate color change from brown to golden yellow. Within 5 minutes, golden crystals of **5** suitable for XRD analysis were obtained in 72% yield. Analysis by  $^1\text{H}$  NMR spectroscopy and elemental analysis indicated **5** is the only product isolated, showing similar reactivity to complex **B**. This suggests that the previously determined unreactive nature of **C** can be circumvented by use of a strong acid, promoting a series of protonation/protonolysis reactions with subsequent N-H heterolysis of  $\text{NH}_3$  to **5**.

### Structural characterization of $\text{N}(\text{SiMe}_3)_2$ -containing complexes

The solid-state molecular structures of complexes **4** and **5** were determined by X-ray diffraction studies. The metrical parameters are presented in Table 1, including those previously reported for complex **B**.

Complex **4** crystallizes in the space group  $P\bar{1}$  with 0.5 molecules per asymmetric unit. Its solid-state structure can be described as an ion pair consisting of two  $\text{BPh}_4^-$  anions and a  $\text{U}^{\text{IV}}/\text{U}^{\text{IV}}$  mixed dication comprising of two  $[(\text{U}^{\text{IV}}(\text{N}(\text{SiMe}_3)_2)(\text{THF})_2)]$  units bridged by two imido ( $\text{NH}^{2-}$ ) ligands. The  $\text{U1}-\text{N1} = 2.198(6)$  Å and  $\text{U1}-\text{N2} = 2.179(5)$  Å bond distances are similar and fully consistent with bridging imido ( $\text{NH}^{2-}$ ) ligands (Fig. 3a).<sup>13i</sup> All distances are consistent with delocalized charge on the uranium ions as indicated by the nearly symmetrical  $\text{U}-\text{N}_{\text{imido}}$  metrical parameters. The protons of the amido ligands can be crystallographically identified, making their assignment unambiguous.

Complex **5** crystallizes in the space group  $P2_1/c$  with one molecule per asymmetric unit. The solid-state molecular structure of **5** shows the presence of an ion pair consisting of three  $\text{BPh}_4^-$  anions and a  $\text{U}^{\text{IV}}/\text{U}^{\text{IV}}$  trication comprising of two  $[(\text{U}^{\text{IV}}(\text{THF})_4)]$  units bridged by one nitrido ( $\text{N}^{3-}$ ) and two amido ( $\text{NH}_2^{1-}$ ) ligands, forming a face-sharing geometry (Fig. 3b). The  $\text{U1}-\text{N1}$  and  $\text{U2}-\text{N1}$  (2.062(3); 2.018(3) Å) bond distances are consistent with the presence of a bridging nitride ( $\mu\text{-N}$ ).<sup>13b</sup> The  $\text{U}-\text{N}-\text{U}$  bond angle changes dramatically from linear in **B** ( $\text{U}-\text{N}-\text{U}$ : 168.97(14)°) to highly bent in the diamond core geometry of **5** (107.41(12)°), and is analogous to the previously reported complex **D** (Scheme 3).<sup>13b,m</sup> The  $\text{U1}-\text{N2} = 2.455(3)$  Å and  $\text{U1}-\text{N3} = 2.449(3)$  Å bond distances are consistent with two bridging amido ( $\text{NH}_2^{1-}$ ) ligands, with nearly symmetrical  $\text{U}-\text{N}_{\text{amido}}$  metrical

parameters. The protons of the  $\text{NH}_2$  ligands can be crystallographically identified, making their assignment unambiguous. The coordination around the  $\text{U}(\text{IV})$  ions is unprecedented for molecular nitride complexes as it contains only solvent molecules and bridging amido ligands, as all ancillary  $-\text{N}(\text{SiMe}_3)_3$  ligands have been removed upon reaction with  $\text{NH}_4\text{BPh}_4$ .

## Conclusion

In summary, we have investigated the reactions of  $\text{H}^+$  and  $\text{NH}_3$  with a series of nitride bridged diuranium(IV) complexes differing in the type and number of supporting ligands.

We found that the nitride ligand is easily protonated by 1.0 equiv. of weak acid ( $\text{HNET}_3\text{BPh}_4$ ) in the  $-\text{OSi}(\text{O}^t\text{Bu})_3$  supported complex **A**, yielding an imido bridged complex **1**. Further protonation of the imido moiety to a terminal  $\text{NH}_3$  complex, **2**, can be achieved by using a large excess of weak acid and longer reaction time, or by means of a stronger acid. These results indicate that the uranium-nitride bond is easily protonated to afford  $\text{NH}_3$ . Ammonia binds the  $\text{U}(\text{IV})$  ion strongly in the resulting mononuclear  $\text{U}-\text{NH}_3$  complex **3**, but can be displaced by addition of strong acid. Furthermore, the  $\text{U}-\text{OSi}(\text{O}^t\text{Bu})_3$  bonds were found to be stable, even in the presence of stronger acids, such as  $\text{NH}_4\text{BPh}_4$ , therefore indicating that  $-\text{OSi}(\text{O}^t\text{Bu})_3$  supporting ligands are well suited for use when acidic conditions are required, such as in the  $\text{H}^+/e^-$  mediated catalytic conversion of  $\text{N}_2$  to  $\text{NH}_3$ .<sup>5j,23</sup>

Conversely, a very different reactivity is observed for both the cationic and anionic nitride bridged complexes, **B** and **C**, supported by  $-\text{N}(\text{SiMe}_3)_2$  ligands. Opposed to complex **A**, the nitride in both **B** and **C** are more resistant toward protonation by acids. For example, when a weak acid, such as  $\text{HNET}_3\text{BPh}_4$ , is employed, the nitride in these complexes is unreactive. This is consistent with the lesser nucleophilic character of the bridging nitride in  $\text{N}(\text{SiMe}_3)_2$ -containing complexes compared to the analogous  $-\text{OSi}(\text{O}^t\text{Bu})_3$  systems, which was also supported by their reactivity toward small molecules ( $\text{CO}$ ,  $\text{CO}_2$  or  $\text{H}_2$ ). Alternatively, addition of the stronger acid,  $\text{NH}_4\text{BPh}_4$ , resulted in the complete loss of  $-\text{N}(\text{SiMe}_3)_2$  supporting ligands, while the bridging nitride remains intact. Moreover, the basic  $-\text{N}(\text{SiMe}_3)_2$  ligands promote the N-H heterolytic cleavage of  $\text{NH}_3$ , yielding a stable bis- $\text{NH}_2$ , mono-nitride bridged complex (**5**), where only ancillary solvent molecules support the metal center. These results demonstrate that basic supporting ligands, such as  $-\text{N}(\text{SiMe}_3)_2$ , present several disadvantages compared to the  $-\text{OSi}(\text{O}^t\text{Bu})_3$  ligands for usage in the development of catalysts for  $\text{N}_2$  conversion to  $\text{NH}_3$ . Utilizing  $\text{OSi}(\text{O}^t\text{Bu})_3$ -containing complexes is not only advantageous for their resistance toward acids, but also for the high reactivity of bound nitrides to yield  $\text{NH}_3$ . In contrast,  $\text{N}(\text{SiMe}_3)_2$ -supported complexes may be of interest for studies pertaining to the heterolytic bond activation of  $\text{NH}_3$ .

## Author contributions

M. K. carried out the synthetic experiments and analysed the experimental data. R. S. carried out the X-ray single crystal structure analyses. M. M. originated the central idea,



coordinated the work, and analysed the experimental data. The manuscript was written through contributions of all authors.

## Conflicts of interest

There are no conflicts to declare.

## Acknowledgements

We acknowledge support from the Swiss National Science Foundation grant number 200021\_178793 and the École Polytechnique Fédérale de Lausanne (EPFL). We thank F. Fadaei-Tirani for important contributions to the X-ray single crystal structure analyses.

## Notes and references

- (a) F. Haber, Ammonia, German patent DE 229126, 1909; (b) F. Haber, *Angew. Chem.*, 1914, **27**, 473–477.
- (a) M. Falcone, L. Chatelain, R. Scopelliti, I. Zivkovic and M. Mazzanti, *Nature*, 2017, **547**, 332–335; (b) P. L. Arnold, T. Ochiai, F. Y. T. Lam, R. P. Kelly, M. L. Seymour and L. Maron, *Nat. Chem.*, 2020, **12**, 654–659; (c) X. Q. Xin, I. Douair, Y. Zhao, S. Wang, L. Maron and C. Q. Zhu, *J. Am. Chem. Soc.*, 2020, **142**, 15004–15011.
- M. Falcone, L. Barluzzi, J. Andrez, F. F. Tirani, I. Zivkovic, A. Fabrizio, C. Corminboeuf, K. Severin and M. Mazzanti, *Nat. Chem.*, 2019, **11**, 154–160.
- (a) I. Korobkov, S. Gambarotta and G. P. A. Yap, *Angew. Chem., Int. Ed.*, 2002, **41**, 3433–3436; (b) N. Jori, L. Barluzzi, I. Douair, L. Maron, F. Fadaei-Tirani, I. Zivkovic and M. Mazzanti, *J. Am. Chem. Soc.*, 2021, **143**(29), 11225–11234.
- (a) D. V. Yandulov and R. R. Schrock, *Science*, 2003, **301**, 76–78; (b) K. Arashiba, Y. Miyake and Y. Nishibayashi, *Nat. Chem.*, 2011, **3**, 120–125; (c) B. Askevold, J. T. Nieto, S. Tussupbayev, M. Diefenbach, E. Herdtweck, M. C. Holthausen and S. Schneider, *Nat. Chem.*, 2011, **3**, 532–537; (d) Y. Nishibayashi, *Nat. Chem.*, 2011, **3**, 502–504; (e) C. J. M. van der Ham, M. T. M. Koper and D. G. H. Hetterscheid, *Chem. Soc. Rev.*, 2014, **43**, 5183–5191; (f) K. Arashiba, E. Kinoshita, S. Kuriyama, A. Eizawa, K. Nakajima, H. Tanaka, K. Yoshizawa and Y. Nishibayashi, *J. Am. Chem. Soc.*, 2015, **137**, 5666–5669; (g) N. B. Thompson, M. T. Green and J. C. Peters, *J. Am. Chem. Soc.*, 2017, **139**, 15312–15315; (h) Y. Ashida, K. Arashiba, K. Nakajima and Y. Nishibayashi, *Nature*, 2019, **568**, 536–540; (i) S. J. K. Forrest, B. Schlusshass, E. Y. Yuzik-Klimova and S. Schneider, *Chem. Rev.*, 2021, **121**, 6522–6587; (j) F. Masero, M. A. Perrin, S. Dey and V. Mougél, *Chem.–Eur. J.*, 2021, **27**, 3892–3928.
- (a) J. J. Scepaniak, J. A. Young, R. P. Bontchev and J. M. Smith, *Angew. Chem., Int. Ed.*, 2009, **48**, 3158–3160; (b) K. C. MacLeod, S. F. McWilliams, B. Q. Mercado and P. L. Holland, *Chem. Sci.*, 2016, **7**, 5736–5746; (c) B. M. Lindley, Q. J. Bruch, P. S. White, F. Hasanayn and A. J. M. Miller, *J. Am. Chem. Soc.*, 2017, **139**, 5305–5308; (d) A. K. Hickey, L. A. Wickramasinghe, R. R. Schrock, C. Tsay and P. Muller, *Inorg. Chem.*, 2019, **58**, 3724–3731.
- T. J. Hebden, R. R. Schrock, M. K. Takase and P. Muller, *Chem. Commun.*, 2012, **48**, 1851–1853.
- F. S. Schendzielorz, M. Finger, C. Volkmann, C. Wurtele and S. Schneider, *Angew. Chem., Int. Ed.*, 2016, **55**, 11417–11420.
- (a) E. Khaskin, M. A. Iron, L. J. W. Shimon, J. Zhang and D. Milstein, *J. Am. Chem. Soc.*, 2010, **132**, 8542–8543; (b) T. Shima and Z. M. Hou, *J. Chem. Soc., Dalton Trans.*, 2010, **39**, 6858–6863; (c) Y. H. Chang, Y. Nakajima, H. Tanaka, K. Yoshizawa and F. Ozawa, *J. Am. Chem. Soc.*, 2013, **135**, 11791–11794; (d) D. V. Gutsulyak, W. E. Piers, J. Borau-Garcia and M. Parvez, *J. Am. Chem. Soc.*, 2013, **135**, 11776–11779; (e) J. R. Khusnutdinova and D. Milstein, *Angew. Chem., Int. Ed.*, 2015, **54**, 12236–12273; (f) M. J. Bezdek, S. Guo and P. J. Chirik, *Science*, 2016, **354**, 730–733; (g) L. Nurdin, Y. Yang, P. G. N. Neate, W. E. Piers, L. Maron, M. L. Neidig, J. B. Lin and B. S. Gelfand, *Chem. Sci.*, 2021, **12**, 2231–2241.
- J. A. H. Frey, G. N. Cloke and S. M. Roe, *Organometallics*, 2015, **34**, 2102–2105.
- (a) D. W. Green and G. T. Reedy, *J. Chem. Phys.*, 1976, **65**, 2921–2922; (b) R. D. Hunt, J. T. Yustein and L. Andrews, *J. Chem. Phys.*, 1993, **98**, 6070–6074; (c) L. Andrews, X. Wang, R. Lindh, B. O. Roos and C. J. Marsden, *Angew. Chem., Int. Ed.*, 2008, **47**, 5366–5370.
- (a) W. J. Evans, S. A. Kozimor and J. W. Ziller, *Science*, 2005, **309**, 1835–1838; (b) G. Nocton, J. Pecaut and M. Mazzanti, *Angew. Chem., Int. Ed.*, 2008, **47**, 3040–3042.
- (a) L. Barluzzi, F. C. Hsueh, R. Scopelliti, B. E. Atkinson, N. Kaltsoyannis and M. Mazzanti, *Chem. Sci.*, 2019, **10**, 3543–3555; (b) S. Fortier, G. Wu and T. W. Hayton, *J. Am. Chem. Soc.*, 2010, **132**, 6888–6889; (c) A. R. Fox, P. L. Arnold and C. C. Cummins, *J. Am. Chem. Soc.*, 2010, **132**, 3250–3251; (d) D. M. King, F. Tuna, E. J. L. McInnes, J. McMaster, W. Lewis, A. J. Blake and S. T. Liddle, *Science*, 2012, **337**, 717–720; (e) D. M. King, F. Tuna, E. J. L. McInnes, J. McMaster, W. Lewis, A. J. Blake and S. T. Liddle, *Nat. Chem.*, 2013, **5**, 482–488; (f) D. M. King and S. T. Liddle, *Coord. Chem. Rev.*, 2014, **266**, 2–15; (g) L. Chatelain, R. Scopelliti and M. Mazzanti, *J. Am. Chem. Soc.*, 2016, **138**, 1784–1787; (h) D. M. King, P. A. Cleaves, A. J. Wooles, B. M. Gardner, N. F. Chilton, F. Tuna, W. Lewis, E. J. L. McInnes and S. T. Liddle, *Nat. Commun.*, 2016, **7**, 13773; (i) L. Barluzzi, L. Chatelain, F. Fadaei-Tirani, I. Zivkovic and M. Mazzanti, *Chem. Sci.*, 2019, **10**, 3543–3555; (j) J. Du, D. M. King, L. Chatelain, F. Tuna, E. J. L. McInnes, A. J. Wooles, L. Maron and S. T. Liddle, *Chem. Sci.*, 2019, **10**, 3738–3745; (k) C. T. Palumbo, L. Barluzzi, R. Scopelliti, I. Zivkovic, A. Fabrizio, C. Corminboeuf and M. Mazzanti, *Chem. Sci.*, 2019, **10**, 8840–8849; (l) L. Barluzzi, R. Scopelliti and M. Mazzanti, *J. Am. Chem. Soc.*, 2020, **142**, 19047–19051; (m) C. T. Palumbo, R. Scopelliti, I. Zivkovic and M. Mazzanti, *J. Am. Chem. Soc.*, 2020, **142**, 3149–3157; (n) M. D. Straub, L. M. Moreau, Y. S. Qiao, E. T. Ouellette, M. A. Boreen, T. D. Lohrey, N. S. Settineri, S. Hohloch, C. H. Booth,





- S. G. Minasian and J. Arnold, *Inorg. Chem.*, 2021, **60**, 6672–6679; (o) L. Maria, I. C. Santos, V. R. Sousa and J. Marcalo, *Inorg. Chem.*, 2015, **54**, 9115–9126.
- 14 (a) A. L. Odom, P. L. Arnold and C. C. Cummins, *J. Am. Chem. Soc.*, 1998, **120**, 5836–5837; (b) P. Roussel and P. Scott, *J. Am. Chem. Soc.*, 1998, **120**, 1070–1071; (c) F. Geoffrey, N. Cloke and P. B. Hitchcock, *J. Am. Chem. Soc.*, 2002, **124**, 9352–9353; (d) W. J. Evans, S. A. Kozimor and J. W. Ziller, *J. Am. Chem. Soc.*, 2003, **125**, 14264–14265; (e) S. M. Mansell, N. Kaltsoyannis and P. L. Arnold, *J. Am. Chem. Soc.*, 2011, **133**, 9036–9051; (f) S. M. Mansell, J. H. Farnaby, A. I. Germeroth and P. L. Arnold, *Organometallics*, 2013, **32**, 4214–4222; (g) P. D. Dau, P. B. Armentrout, M. C. Michelini and J. K. Gibson, *Phys. Chem. Chem. Phys.*, 2016, **18**, 7334–7340; (h) M. Falcone, L. Chatelain and M. Mazzanti, *Angew. Chem., Int. Ed.*, 2016, **55**, 4074–4078; (i) M. Falcone, C. E. Kefalidis, R. Scopelliti, L. Maron and M. Mazzanti, *Angew. Chem., Int. Ed.*, 2016, **55**, 12290–12294; (j) M. D. Walter, *Adv. Organomet. Chem.*, 2016, **65**, 261–377; (k) P. A. Cleaves, C. E. Kefalidis, B. M. Gardner, F. Tuna, E. J. L. McInnes, W. Lewis, L. Maron and S. T. Liddle, *Chem.–Eur. J.*, 2017, **23**, 2950–2959; (l) M. Falcone, L. N. Poon, F. F. Tirani and M. Mazzanti, *Angew. Chem., Int. Ed.*, 2018, **57**, 3697–3700; (m) E. Lu, B. E. Atkinson, A. J. Wooles, J. T. Boronski, L. R. Doyle, F. Tuna, J. D. Cryer, P. J. Cobb, I. J. Vitorica-Yrezabal, G. F. S. Whitehead, N. Kaltsoyannis and S. T. Liddle, *Nat. Chem.*, 2019, **11**, 806–811; (n) M. A. Boreen, G. D. Rao, D. G. Villarreal, F. A. Watt, R. D. Britt, S. Hohloch and J. Arnold, *Chem. Commun.*, 2020, **56**, 4535–4538; (o) L. Chatelain, E. Louyriac, I. Douair, E. L. Lu, F. Tuna, A. J. Wooles, B. M. Gardner, L. Maron and S. T. Liddle, *Nat. Commun.*, 2020, **11**, 337; (p) D. Singh, W. R. Buratto, J. F. Torres and L. J. Murray, *Chem. Rev.*, 2020, **120**, 5517–5581; (q) L. Barluzzi, F. C. Hsueh, R. Scopelliti, B. E. Atkinson, N. Kaltsoyannis and M. Mazzanti, *Chem. Sci.*, 2021, **12**, 8096–8104.
- 15 (a) R. K. Thomson, T. Cantat, B. L. Scott, D. E. Morris, E. R. Batista and J. L. Kiplinger, *Nat. Chem.*, 2010, **2**, 723–729; (b) P. L. Arnold, M. W. McMullon, J. Rieb and F. E. Kuhn, *Angew. Chem., Int. Ed.*, 2015, **54**, 82–100; (c) K. C. Mullane, H. Ryu, T. Cheisson, L. N. Grant, J. Y. Park, B. C. Manor, P. J. Carroll, M. H. Baik, D. J. Mindiola and E. J. Schelter, *J. Am. Chem. Soc.*, 2018, **140**, 11335–11340; (d) M. Yadav, A. J. Metta-Magana and S. Fortier, *Chem. Sci.*, 2020, **11**, 2381–2387.
- 16 C. Camp, J. Pecaut and M. Mazzanti, *J. Am. Chem. Soc.*, 2013, **135**, 12101–12111.
- 17 D. K. Modder, C. T. Palumbo, I. Douair, R. Scopelliti, L. Maron and M. Mazzanti, *Chem. Sci.*, 2021, **12**, 6153–6158.
- 18 D. K. Modder, C. T. Palumbo, I. Douair, F. Fadaei-Tirani, L. Maron and M. Mazzanti, *Angew. Chem., Int. Ed.*, 2021, **60**, 3737–3744.
- 19 D. A. Johnson, J. C. Taylor and A. B. Waugh, *J. Inorg. Nucl. Chem.*, 1979, **41**, 827–831.
- 20 S. S. Rudel, H. L. Deubner, M. Muller, A. J. Karttunen and F. Kraus, *Nat. Chem.*, 2020, **12**, 962–967.
- 21 D. M. King, J. McMaster, F. Tuna, E. J. L. McInnes, W. Lewis, A. J. Blake and S. T. Liddle, *J. Am. Chem. Soc.*, 2014, **136**, 5619–5622.
- 22 J. A. H. Frey, G. N. Cloke and S. M. Roe, *Organometallics*, 2015, **34**, 2102–2105.
- 23 M. J. Chalkley, M. W. Drover and J. C. Peters, *Chem. Rev.*, 2020, **120**, 5582–5636.

